

Excess heat and local thermodynamic quantities in heat-conducting systems

Yoshiyuki Chiba and Naoko Nakagawa

(Dated: October 4, 2018)

We examined numerically entropy extended to heat-conducting systems, whose difference is equal to the excess entropy production determined from the excess heat absorbed from the environment. We found that the entropy determined by the excess heat well coincides with the spatial integration of the local entropies determined according to the local equilibrium hypothesis, coinciding not only in the thermodynamic limit but also in small systems with a huge finite-size effect. In sufficiently large systems as well as at equilibrium, the entropy exhibits both extensive and additive properties; however, the two properties do not degenerate each other differently from those at equilibrium.

PACS numbers: 05.70.Ln, 05.40.-a, 05.60.Cd

The extension of thermodynamics from equilibrium to nonequilibrium states has been a goal for a long time, and several attempts to extend equilibrium thermodynamics to nonequilibrium steady states (NESS), called steady-state thermodynamics (SST) [1–4], have been made. In SST, thermodynamic relations such as the Clausius relation and maximum work principle are extended to the transition between two NESS, which leads to a definition of thermodynamic functions in NESS [5–13].

In several nonequilibrium systems, the idea of local equilibrium has been successful. Various phenomena can be explained by adopting local thermodynamic quantities such as local temperature or density, as is exemplified in fluid turbulence. The extended thermodynamic functions to NESS should be consistent with the local equilibrium quantities for such phenomena. To examine the correspondence to the local equilibrium could be a good test for the proposed thermodynamic functions for NESS.

Taking note of the entropy proposed in [6], which is directly connected to an observable—the so-called excess heat, we focus on heat-conducting systems and determine the entropy extended to NESS by measuring heat in numerical experiments. Comparing it with the entropy deduced from local equilibrium hypothesis, we find good correspondence between the two entropies not only for the systems in the thermodynamic limit but also for those with rather small sizes. Because the excess heat is a global quantity measured just at the boundaries of the system, this correspondence offers new experimental possibilities for small systems in which accessing local quantities is difficult. In the thermodynamic limit, the entropy for the heat-conducting states is found to possess both extensive and additive properties, however, the two properties are not unified.

Model: As a model system for performing numerical experiments, we adopt a one-dimensional heat-conducting lattice. We shall take the ϕ^4 model, which is known to exhibit normal heat conduction obeying

Fourier's law [14]. Its Hamiltonian is written as

$$H(\{x\}, \{p\}) = \sum_{i=1}^L \left(\frac{p_i^2}{2} + \frac{x_i^4}{4} \right) + \sum_{i=1}^{L-1} \frac{(x_{i+1} - x_i)^2}{2}, \quad (1)$$

where x_i and p_i are the deviation from the equilibrium position and the momentum for the i th site, and L is the number of elements in the lattice. The two ends, $i = 1$ and L , of the lattice are in contact with heat baths of T_1^b and T_2^b , respectively. The evolution equation of each element is given by the canonical equations for the bulk ($2 \leq i \leq L - 1$) and the Langevin equation for the two ends:

$$\dot{p}_1 = -\frac{\partial H}{\partial x_1} - \gamma p_1 + \sqrt{2\gamma T_1^b(t)} \circ \xi_1(t), \quad \dot{x}_1 = p_1, \quad (2)$$

$$\dot{p}_i = -\frac{\partial H}{\partial x_i}, \quad \dot{x}_i = p_i, \quad (3)$$

$$\dot{p}_L = -\frac{\partial H}{\partial x_L} - \gamma p_L + \sqrt{2\gamma T_2^b(t)} \circ \xi_2(t), \quad \dot{x}_L = p_L \quad (4)$$

where \circ means Stratonovich's multiplier and k_B is taken as unity. $\xi_k(t)$ is a Gaussian white noise satisfying $\langle \xi_k(t) \rangle = 0$ and $\langle \xi_k(t) \xi_{k'}(t') \rangle = \delta_{kk'} \delta(t - t')$. We set $\gamma = 1$.

Observables: We measure the heat flow $j_k(t)$ from the k th heat bath to the lattice. Adopting stochastic energetics [15], we define

$$j_1(t) := p_1 \circ \left(-\gamma p_1 + \sqrt{2\gamma T_1^b(t)} \circ \xi_1(t) \right), \quad (5)$$

$$j_2(t) := p_L \circ \left(-\gamma p_L + \sqrt{2\gamma T_2^b(t)} \circ \xi_2(t) \right). \quad (6)$$

When we fix $T_1^b(t)$ and $T_2^b(t)$ as T_1^b and T_2^b and relax the system sufficiently long, the system reaches a unique steady state with steady heat flow $J^{\text{st}}(T_1^b, T_2^b, L) := \langle j_1 \rangle = -\langle j_2 \rangle$, where $\langle \cdot \rangle$ is the ensemble and/or long-time average.

The entropy production rates in the baths are defined as

$$\theta(t) := -\frac{j_1(t)}{T_1^b(t)} - \frac{j_2(t)}{T_2^b(t)}, \quad (7)$$

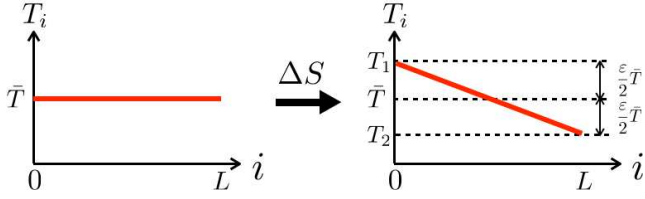


FIG. 1: Sketch of the temperature profile before the change (initial equilibrium state) and the final heat-conducting state. To determine the entropy in the heat-conducting state (right), we apply a protocol to change the temperature of the heat baths from (\bar{T}, \bar{T}) to (T_1, T_2) . We fix $\bar{T} = \frac{T_1 + T_2}{2}$.

which can be decomposed to steady and excess ones as

$$\theta_{\text{st}}(t) := -J^{\text{st}}(T_1^{\text{b}}(t), T_2^{\text{b}}(t), L) \left(\frac{1}{T_1^{\text{b}}(t)} - \frac{1}{T_2^{\text{b}}(t)} \right), \quad (8)$$

$$\theta_{\text{ex}}(t) := \theta(t) - \theta_{\text{st}}(t). \quad (9)$$

Consistently with the second law of thermodynamics, the steady part θ_{st} is always non-negative, whereas the time-dependent part θ_{ex} is not necessarily bounded to non-negative values. θ_{ex} is produced by an external operation.

In the following parts, we treat the change of entropy from an equilibrium state at $T_1^{\text{b}} = T_2^{\text{b}} = \bar{T}$ to a heat-conducting state with $T_1^{\text{b}} = T_1 = (1 + \frac{\varepsilon}{2})\bar{T}$ and $T_2^{\text{b}} = T_2 = (1 - \frac{\varepsilon}{2})\bar{T}$. See Fig. 1. $\varepsilon = (T_1 - T_2)/\bar{T}$ is a nondimensional parameter used to indicate the degree of nonequilibrium in the final heat-conducting state.

The change of entropy from iso-thermal to heat-conducting states is connected to the excess entropy production via the extended Clausius equality as derived in [6]. It is given by

$$S_{\text{neq}}(L, \bar{T}, \varepsilon) - S_{\text{eq}}(L, \bar{T}) + \Theta_{\text{ex}} = O(\varepsilon^3), \quad (10)$$

which is valid in quasi-static operations. Here Θ_{ex} is the excess entropy production in the two heat baths,

$$\Theta_{\text{ex}} = \int_0^\tau \langle \theta_{\text{ex}}(t) \rangle dt, \quad (11)$$

for the observation in a period $[0, \tau]$. Equality (10) offers an experimental method to determine the entropy in the heat-conducting states by measuring the heat currents. By utilizing (10) we can examine the properties of the nonequilibrium entropy.

Local equilibrium as a reference: We assume that the local temperature corresponds to the kinetic temperature for each i th site as

$$T_i = \langle p_i^2 \rangle. \quad (12)$$

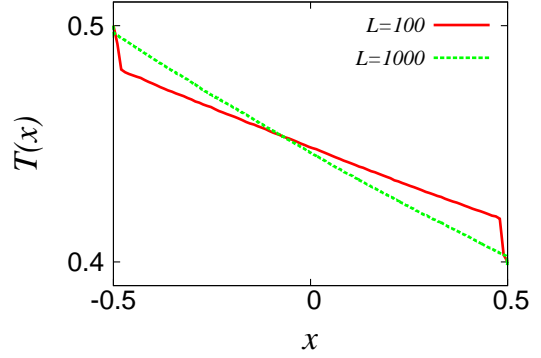


FIG. 2: Temperature profile at $L = 100$ and 1000 in the scaled space $x = \frac{i}{L} - \frac{1}{2}$. $(T_1, T_2) = (0.5, 0.4)$, which corresponds to $(\bar{T}, \varepsilon) = (0.45, 0.222)$. For small lattices such as $L = 100$, greater gaps of the temperature at both boundaries exist and the slope in the bulk is lower. The gaps become smaller and the slope becomes almost $(T_1 - T_2)/L$ for larger lattices exemplified by $L = 1000$.

From the hypothesis of local equilibrium, we define the entropy for the entire system as,

$$S_{\text{leq}}(L, \bar{T}, \varepsilon) = \sum_{i=1}^L s_i, \quad s_i = c \log T_i, \quad (13)$$

where s_i is the local entropy derived from $ds_i = du_i/T_i$ with local internal energy $u_i = cT_i$, and c is the specific heat in equilibrium, whose value is determined by numerical simulation of Eqs. (2), (3), and (4). We obtained $c \simeq 0.88$ for a wide range of temperature, which is consistent with the reported value of 0.86 for a sufficiently long lattice [14].

In thermodynamic limit, we can apply the equation of heat conduction to obtain the temperature profile for the steady states. We start from the heat conductivity $\lambda(T)$, which satisfies $J^{\text{st}} = -\lambda(T)\nabla T$. Our numerical simulation suggests that $\lambda(T) = \lambda_0 T^{-4/3}$, with a constant λ_0 for sufficiently large systems. The functional form is consistent with the previous report in [16]. Solving the heat-conduction equation with the boundary condition $T(x = -\frac{1}{2}) = (1 + \frac{\varepsilon}{2})\bar{T}$ and $T(x = \frac{1}{2}) = (1 - \frac{\varepsilon}{2})\bar{T}$, we obtain the temperature profile as $T(x) = \left[1 - \varepsilon x + \frac{2\varepsilon^2}{3} (x^2 - \frac{1}{4}) \right] \bar{T} + O(\varepsilon^3)$, where $x = \frac{i}{L} - \frac{1}{2}$. Thus, we have the local entropy $s(x) = c \log T(x)$ for the thermodynamic limit. Integrating the local entropy $s(x)$ over the space as $S_{\text{leq}} = L \int_{-1/2}^{1/2} s(x) dx$, gives the following estimate of entropy:

$$S_{\text{leq}}(L, \bar{T}, \varepsilon) \xrightarrow{L \rightarrow \infty} S_{\text{eq}}(L, \bar{T}) - \frac{11}{72} c L \varepsilon^2 + O(\varepsilon^3), \quad (14)$$

which indicates that ΔS_{leq} is independent of \bar{T} and is proportional to $\varepsilon^2 L$.

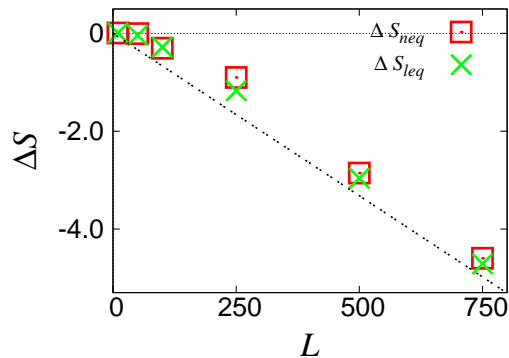


FIG. 3: System size dependence of the entropy difference ΔS_{neq} and ΔS_{leq} for the change (\bar{T}, \bar{T}) to (T_1, T_2) . (T_1, T_2) is fixed to $(0.5, 0.4)$ whereas $L = 10, 50, 100, 250, 500, 750$. The error bar is smaller than the size of each point. The dotted line corresponds to the thermodynamic limit in Eq. (14). Note that ΔS_{neq} agrees with ΔS_{leq} even for the smallest L .

The numerically obtained temperature profile agrees with the estimated $T(x)$ well in the sufficiently long lattice, as is exemplified by the $L = 1000$ line in Fig. 2. The profile begins to exhibit gaps in temperature as shown in the $L = 100$ line in the same figure. These gaps are a result of the finite-size effect in the ϕ_4 model, as is discussed in [14].

Numerical results for nonequilibrium entropy: We demonstrate the numerical results for $\Delta S_{\text{neq}} := S_{\text{neq}}(L, \bar{T}, \varepsilon) - S_{\text{eq}}(L, \bar{T})$ and $\Delta S_{\text{leq}} := S_{\text{leq}}(L, \bar{T}, \varepsilon) - S_{\text{eq}}(L, \bar{T})$. The scheme used to determine these differences is reported in *Appendix*, in which we explain effective method to measure S_{neq} by applying the protocols of finite speed.

In Fig. 3, we plot ΔS_{neq} and ΔS_{leq} obtained by varying the size L of the lattice for fixed \bar{T} and ε . Figure 4 shows ΔS_{neq} for various values of ε and \bar{T} with $L = 500$. In both figures, we find a coincidence of the two entropy differences, $\Delta S_{\text{neq}} \simeq \Delta S_{\text{leq}}$, i.e.,

$$S_{\text{neq}}(L, \bar{T}, \varepsilon) \simeq S_{\text{leq}}(L, \bar{T}, \varepsilon), \quad (15)$$

over the values of L and ε . ΔS_{leq} and ΔS_{neq} tend to converge to the dotted line as L becomes large, which corresponds to the thermodynamic limit of ΔS_{leq} in Eq. (14) resulting from the heat-conduction equation.

Note that there exist gaps in temperature at the boundaries of the lattice, as is shown in Fig. 2. They are a typical finite-size effect, becoming smaller as the size L increases and vanishing in the thermodynamic limit. Figure 3 shows that S_{neq} coincides with S_{leq} regardless of the size of the gaps; i.e., their coincidence is barely disturbed by the finite-size effect.

As shown in Fig. 4, ΔS_{neq} is almost proportional to ε^2 independently of \bar{T} . ΔS_{leq} seems to deviate more from the thermodynamic limit (dotted line) as ε be-

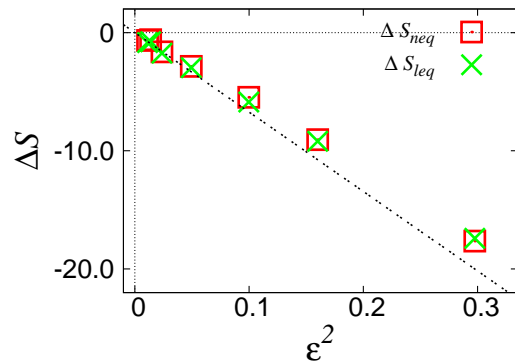


FIG. 4: The dependence of the degree ε of nonequilibrium for the entropy difference ΔS_{neq} and ΔS_{leq} for $L = 500$. The error bar is smaller than the size of each point. $(T_1, T_2) = (0.5, 0.45), (0.45, 0.4), (0.5, 0.6), (0.55, 0.4), (0.6, 0.4), (0.7, 0.4)$. The dotted line corresponds to the thermodynamic limit in Eq. (14). The deviation from the thermodynamic limit grows as ε increases, while the coincidence $\Delta S_{\text{neq}} \simeq \Delta S_{\text{leq}}$ has been maintained.

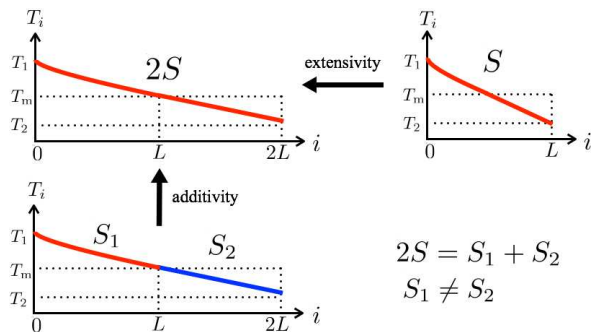


FIG. 5: Schematic figure to explain the difference between extensivity and additivity in heat-conducting states.

comes larger. This is attributable to certain finite-size effects because the temperature profile converges to the estimated thermodynamic limit for sufficiently large L , which means the convergence of ΔS_{leq} to (14).

Extensivity and additivity for the nonequilibrium entropy: In equilibrium thermodynamics, extensivity and additivity of thermodynamic functions are one of the most important properties. They are essential for the variational principles in thermodynamics, for instance. We here notice to these two properties for the entropy S_{neq} extended to NESS. As shown in Fig. 3, we obtain

$$S_{\text{neq}}(L, \bar{T}, \varepsilon) \propto L \quad (16)$$

for sufficiently large lattices, which means that the entropy S_{neq} is an extensive variable in the thermodynamic limit under the fixed ε . Because S_{neq} is equal to the sum S_{leq} of the local entropies in Eq. (13), it is expected to

be additive even in NESS. In what follows, we examine the relation of its additivity to its extensivity in the heat-conducting states.

The additive system is allowed to be divided into parts without changing its local properties. To divide the system, we need to attach new heat baths at the new ends to keep the temperature profile. The temperature gap at the new ends is inconsistent with the original smooth profile so that we require the system to be in the thermodynamic limit for holding the additivity.

We demonstrate the additivity for the separation of the system into two parts as exemplified in Fig. 5, where we notate $S(L, T_1, T_2) := S_{\text{neq}}(L, \bar{T}, \varepsilon)$ to emphasize the boundary conditions to drive the system to NESS. Here $\bar{T} = \frac{T_1+T_2}{2}$ and $\varepsilon = \frac{T_1-T_2}{T}$. We attach new heat baths of T_m at the new two ends of $x = 0$, i.e. $i = L/2$, where $T_m := T(x = 0) = (1 - \frac{\varepsilon^2}{6})\bar{T} + O(\varepsilon^3)$ as assigned by the steady solution of the heat-conduction equation. From (14), we have $S(L, T_1, T_m) = S_{\text{eq}}(L, (1 + \frac{\varepsilon}{4} - \frac{\varepsilon^2}{12})\bar{T}) - \frac{11}{72}cL\frac{\varepsilon^2}{4} + O(\varepsilon^3)$ and $S(L, T_m, T_2) = S_{\text{eq}}(L, (1 - \frac{\varepsilon}{4} - \frac{\varepsilon^2}{12})\bar{T}) - \frac{11}{72}cL\frac{\varepsilon^2}{4} + O(\varepsilon^3)$. It is remarkable that $S(L, T_1, T_m) \neq S(L, T_m, T_2)$ due to the difference in S_{eq} .

Using $S_{\text{eq}}(L, T) = cL \log T$, the sum is estimated as $S(L, T_1, T_m) + S(L, T_m, T_2) = 2cL \log \bar{T} - \frac{11}{36}cL\varepsilon^2 + O(\varepsilon^3)$, whose right hand side is equal to $S_{\text{neq}}(2L, \bar{T}, \varepsilon)$ in the precision of ε^2 , which is written as $S(2L, T_1, T_2)$. Thus we obtain the additivity such that

$$S(2L, T_1, T_2; J) = S(L, T_1, T_m; J) + S(L, T_m, T_2; J), \quad (17)$$

where we specified the steady heat current J to prepare the next discussion.

The extensivity (16) concluded for the heat-conducting states is explicitly written as

$$S(aL, T_1, T_2; J) = aS(L, T_1, T_2; J/a), \quad (18)$$

which is valid in the thermodynamic limit. Compared the terms in (17) with the term in (18) for $a = 2$, it is obvious that $S(L, T_1, T_2; J/2) \neq S(L, T_1, T_m; J)$ nor $S(L, T_m, T_2; J)$. This is in contrast to equilibrium states, where the additivity is degenerate to the extensivity because $S(L_1, T) = S(L_2, T)$ when $L_1 = L_2$.

Summarizing the above, the entropy for heat-conducting states is characterized by its extensivity and additivity as well as equilibrium states. The two properties hold in the thermodynamic limit in which the system does not exhibit any boundary effect although the extensivity does not degenerate to the additivity. This is a significant difference between equilibrium and nonequilibrium entropy.

Discussion: We performed numerical experiments to determine the nonequilibrium entropy S_{neq} for heat-conducting states in one-dimensional lattices exhibiting Fourier's law. We discovered that S_{neq} determined from

the excess heat currents coincides with S_{leq} determined according to the local equilibrium hypothesis. As is well known, various nonequilibrium phenomena have been explained by local thermodynamic quantities, which are expressed by the differentials of the local equilibrium entropy. Our finding suggests that local thermodynamic quantities become accessible by measuring excess heat, which is a global quantity measured just at the boundaries of the system.

In equilibrium, extensivity and additivity are degenerated and not distinguished. We confirmed the two properties to be extended to heat-conducting states, but we simultaneously found the breakdown of the degeneration. Thus, we question whether the conventional logic in thermodynamics can be applied to nonequilibrium. For instance, Sasa and Tasaki [3] discussed extensivity and additivity for NESS to apply variational principle to their nonequilibrium free energy, however, the breakdown of the degeneration did not seem to be recognized.

The extensivity (18) and the additivity (17) coincides with those formulated by Bodineau and Derrida [18], which were introduced in the large deviation functional for the current fluctuations. This coincidence may suggest that their free energy is related to S_{neq} and the excess heat.

In the extended Clausius relation (10), S_{neq} is known to be represented by symmetrized Shannon entropy $-\langle \log \sqrt{\rho_{\text{st}}(\Gamma)\rho_{\text{st}}(\Gamma^*)} \rangle$, where $\rho_{\text{st}}(\Gamma)$ and $\rho_{\text{st}}(\Gamma^*)$ are the stationary distribution of microstates $\Gamma = (\{x\}, \{p\})$ and $\Gamma^* = (\{x\}, -\{p\})$. Our results suggest that both $\rho_{\text{st}}(\Gamma)$ and $\rho_{\text{st}}(\Gamma^*)$ are approximately decomposed into local canonical distributions; therefore, S_{neq} can be represented by Shannon entropy as well as in equilibrium systems. In strongly correlated systems with long-range interactions where the local equilibrium hypothesis is not valid, S_{neq} might be distinct from Shannon entropy.

Aoki and Kusnezov reported a long-range correlation of the local quantities for the ϕ^4 model for much larger ε values than those that we used [19]. To investigate the long-range correlations by means of the excess heat measurement, we need to improve the theory. This is because we will require a precision of $O(\varepsilon^4)$ for S_{neq} to include the effect of the long-range correlations, whereas the present excess heat measurement estimates the entropy to the precision of $O(\varepsilon^2)$. This remains as a future project.

Acknowledgement: We are grateful to Keiji Saito for useful comments and suggestions. This work was supported by KAKENHI Nos. 15K05196 and 25103002.

APPENDIX

Effective methods to measure entropy differences ΔS_{neq} : To determine ΔS_{neq} , we measure entropy production in heat baths according to Eq. (10). Note that this is valid in quasi-static operations, for which mea-

measurements are difficult to make experimentally. As an effective way to estimate ΔS_{neq} , we utilize

$$S_{\text{neq}}(L, \bar{T}, \varepsilon) - S_{\text{eq}}(L, \bar{T}) = -\frac{1}{2}(\Theta - \Theta^\dagger) + O(\varepsilon^3) \quad (19)$$

instead of Eq. (10). This is the relation for a *pair of one-step protocols*, called forward and backward protocols (see Fig. 6). Equation (19) offers the same accuracy for ΔS_{neq} with (10), i.e., the error of $O(\varepsilon^3)$, without applying quasi-static operations as explained follow. In [17], the same method was applied to determine S_{neq} numerically, however, the method was not fully argued.

When we apply a protocol of a finite speed to change the states as shown in Fig. 1, we have $\Delta S_{\text{neq}} + \Theta_{\text{ex}} = O(\delta^2) + O(\varepsilon^3)$ instead of (10), where δ represents the size of the change, i.e., $\delta = O(\varepsilon)$. Note that the error of $O(\delta^2)$ could become larger than that of the quasi-static protocol of $O(\varepsilon^3)$ in general.

We here estimate the error in a stepwise protocol as shown in Fig. 6. By using the formulae given in section 3.3 of [7], the error is written as

$$\int d\Gamma \frac{\Delta \rho_{\text{st}}(\Gamma) \Delta \rho_{\text{st}}(\Gamma^*)}{\rho_{\text{st}}(\Gamma)} + O(\varepsilon^2 \delta, \varepsilon \delta^2, \delta^3), \quad (20)$$

where $\rho_{\text{st}}(\Gamma)$ and $\rho_{\text{st}}(\Gamma^*)$ are the initial (or final) stationary distribution of microstates $\Gamma = (\{x\}, \{p\})$ and $\Gamma^* = (\{x\}, -\{p\})$. $\Delta \rho_{\text{st}}(\Gamma)$ is the difference of $\rho_{\text{st}}(\Gamma)$ produced by the protocol.

Because the error (20) in the forward protocol is equal to that in the backward protocol in the precision of $O(\delta^2)$, we can cancel the error of $O(\delta^2)$ by combining the products of two protocols. Thus, the dominant error in (19) becomes $O(\varepsilon^3)$, which is the same order as the error in (10).

Measurement of ΔS_{neq} : For applying (19), we measure the two entropy productions Θ and Θ^\dagger for the forward and backward protocols, respectively. We prepare the equilibrium ensemble at \bar{T} to start the forward protocol in Fig. 6. Taking this as an initial ensemble at $t = 0$, we integrate (2), (3), and (4). We abruptly change the temperature of the two heat baths at $t = \tau$ and continue the integration up to 2τ , where τ is much longer than the system's relaxation time. We measure the heat currents $j_1(t)$ and $j_2(t)$ along each trajectory, and take their ensemble averages to form $\Theta = -\int_\tau^{2\tau} dt (\langle j_1(t) \rangle / T_1 + \langle j_2(t) \rangle / T_2)$. The contribution in $[0, \tau]$ is assumed to be vanishing because it is in equilibrium states.

The procedure is almost the same in the backward protocol except for the initial ensemble which should be prepared in the steady heat-conducting states. For the backward protocol, we prepare the steady heat-conducting state of T_1 and T_2 and then change both temperatures into \bar{T} simultaneously at $t = \tau$. We measure the entropy production $\Theta^\dagger = -\int_0^\tau dt (\langle j_1(t) \rangle / T_1 + \langle j_2(t) \rangle / T_2) -$

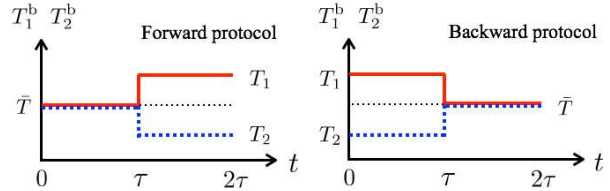


FIG. 6: Pair of protocols to estimate ΔS_{neq} by utilizing (19). The heat baths T_1^b and T_2^b are changed in a stepwise manner as is indicated by red and blue dotted lines, respectively. The forward and backward protocols are exactly time-reversed. The period τ is set to be much longer than the typical relaxation time.

$\int_\tau^{2\tau} dt (\langle j_1(t) \rangle + \langle j_2(t) \rangle) / \bar{T}$. The first integral gives the steady entropy production, which cancels the same contribution included in Θ . The second corresponds to the excess entropy production induced by the change from heat-conducting to equilibrium states.

Measurement of ΔS_{leq} : To obtain ΔS_{leq} , we calculate both $S_{\text{leq}}(L, \bar{T}, \varepsilon)$ in the steady heat-conducting state and $S_{\text{eq}}(L, \bar{T})$ in the equilibrium state. In each steady state, we estimate the local kinetic temperature T_i by a long-time and/or ensemble average and then calculate s_i by applying (13). Summing up the local entropy s_i over the lattice, we obtain the global entropy $S_{\text{leq}}(L, \bar{T}, \varepsilon)$ and $S_{\text{eq}}(L, \bar{T})$ in the respective steady states.

-
- [1] R. Landauer, Phys. Rev. A **18**, 255-266 (1978).
 - [2] Y. Oono and M. Paniconi, Prog. Theor. Phys. Suppl. **130**, 29 (1998).
 - [3] S.-i. Sasa and H. Tasaki, J. Stat. Phys. **125**, 125–224 (2006).
 - [4] D. Ruelle, Proc. Natl. Acad. Sci. U.S.A. **100**, 3054–3058 (2003).
 - [5] T. Hatano and S.-i. Sasa, Phys. Rev. Lett. **86**, 3463 (2001).
 - [6] T. S. Komatsu, N. Nakagawa, S.-i. Sasa and H. Tasaki, Phys. Rev. Lett. **100**, 230602 (2008).
 - [7] T. S. Komatsu, N. Nakagawa, S.-i. Sasa and H. Tasaki, J. Stat. Phys. **142**, 127–153 (2011).
 - [8] K. Saito and H. Tasaki, J. Stat. Phys. **145**, 1275–1290 (2011).
 - [9] N. Nakagawa, Phys. Rev. E **85**, 051115 (2012).
 - [10] T. S. Komatsu, N. Nakagawa, S. -i. Sasa and H. Tasaki, J. Stat. Phys. **158**, 1195-1414 (2015).
 - [11] L. Bertini, D. Gabrielli, G. Jona-Lasinio, and C. Landim, Phys. Rev. Lett. **110**, 020601 (2013).

- [12] C. Maes and K. Netocny, *J. Stat. Phys.* **154**, 188–203 (2014).
- [13] S.-I. Sasa, *J. Stat. Mech.* P01004 (2014).
- [14] K. Aoki and D. Kusnezov, *Annals of Physics* **295**, 5080 (2002)
- [15] K. Sekimoto, *Stochastic Energetics* (Springer, Berlin, 2010), K. Sekimoto, *J. Phys. Soc. Jpn.* **66**, 1234 (1997).
- [16] K. Aoki and D. Kusnezov, *Phys. Lett. A* **265**, 250 (2000).
- [17] T. S. Komatsu, N. Nakagawa, S. Sasa, H. Tasaki and N. Ito, *Prog. Theor. Phys. Suppl.* **184**, 329 (2010)
- [18] T. Bodineau and B. Derrida, *Phys. Rev. Lett.* **92**, 180601 (2004).
- [19] K. Aoki and D. Kusnezov, *Phys. Lett. A* **309**, 377 (2003).